



Sediment generation on a volcanic island with arid tropical climate: A perspective based on geochemical maps of topsoils and stream sediments from Santiago Island, Cape Verde[☆]



Marina M.S. Cabral Pinto ^a, Pedro A. Dinis ^{b,*}, Maria M.V.G. Silva ^c, Eduardo A. Ferreira da Silva ^d

^a Geobiotec Research Centre and CNC, Department of Earth Sciences, University of Coimbra, 3030-790 Coimbra, Portugal

^b MARE - Marine and Environmental Sciences Centre, Department of Earth Sciences, 3030-790, Coimbra, Portugal

^c CEMUC, Department of Earth Sciences, University of Coimbra, 3030-790 Coimbra, Portugal

^d University of Aveiro, Department of Geosciences, Geobiotec Research Centre, 3810-193 Aveiro, Portugal

ARTICLE INFO

Article history:

Received 1 September 2016

Received in revised form

20 October 2016

Accepted 27 October 2016

Available online 31 October 2016

Keywords:

Volcanic island

Santiago Island (Cape Verde)

Topsoils

Bedload stream sediments

Weathering

Erosion

ABSTRACT

The present research tests the application of geochemical atlas of soils and stream sediments in the investigation of weathering and erosion processes on volcanic islands. The composition of surface soils collected in six catchments from Santiago Island (Cape Verde) are compared with bedload stream deposits sourced by these catchment areas in order to evaluate the spatial variability of these exogenous processes. The geochemistry of bedload stream deposits is between that of the fresh rocks and the topsoils of their source areas. Relative to average soil composition, bedload deposits are depleted in most of less-mobile elements (e.g., Al, Fe, La, Sc) and strongly enriched in Na and, usually, Ca. When the topsoil weathering intensity in the catchment areas is highly variable and the composition of bedload deposits is substantially different from the average soil composition, bedload deposits should incorporate significant amounts of poorly-weathered rocks and sectors from erosion occur within the drainage basin. Ratios of non-mobile elements allow the identification of highly vulnerable and erosion-protected sectors within the catchments. It is proposed that the catchments of the rivers in the SW flanking side of Santiago Island include sectors where lava shields formed during the post-erosional eruptive phases are capable of an effective protection to erosion. Conversely, the NE-facing part of the island is highly dissected and any younger post-erosional cover was either completely eroded away, or never existed in the first place. Simple compositional parameters derived from the databases of geochemical maps of soil and stream sediments provide important information for the analyses of weathering, erosion and denudation processes at the catchment scale.

© 2016 Elsevier Ltd. All rights reserved.

1. Introduction

Mapping focused on the detection of geochemical anomalies was initially designed for mineral exploration (Nichol et al., 1966; Levinson, 1974). These maps also provide relevant information on the natural state of the environment. Thus, geochemical surveys focused on soil and stream sediment compositions were used in the investigations of anthropogenic pollution (Darnley et al., 1995; Plant et al., 2001; Albanese et al., 2007; Cabral Pinto et al., 2012)

and medical geology (Reimann et al., 2003; Komatina, 2004; Cheng et al., 2008; Cabral Pinto et al., 2014). In view of their application in different fields, geochemical atlases of soils and stream sediment have been prepared for numerous regions worldwide (Rapant et al., 1999; Lima et al., 2005; Albanese et al., 2007; Inácio et al., 2008; de Caritat and Cooper, 2011; Cabral Pinto, 2010; Rawlins et al., 2012; Martin et al., 2016).

The composition of fluvial deposits is determined by the geology of the source area and several transformations during the sediment cycle (sorting, mineral disintegration, transitory weathering etc.) that may shift the final sediment compositions from their parent regolith (e.g., Johnsson, 1993). If the transformations related to hydraulic sorting and mechanical selection are not significant, the

[☆] This paper has been recommended for acceptance by Prof. M. Kersten.

* Corresponding author.

E-mail address: pdinis@dct.uc.pt (P.A. Dinis).

composition of fluvial deposits is expected to reflect the average volumetric contributions of different geological units within their drainage basins (Ingersoll, 1990; Arribas and Tortosa, 2003; Weltje, 2012). A combined analysis of fluvial sediments and soils collected in the respective catchments has the potential of giving relevant information about the relative volumetric contribution of detritus derived from different locations within the watersheds. An analysis of the dissolved load, suspended load and bedload, along with a comparison with the composition of the rocks of drainage areas, was applied in studies of the denudation rates and sediment yields of volcanic islands (Louvat and Allègre, 1997, 1998; Rad et al., 2006, 2007; Nelson et al., 2013). However, as far as we know, data from a geochemical atlas of soil and stream sediments were never used to investigate the processes of regolith erosion and sediment generation in these settings. Volcanic islands in semi-arid setting are under strong erosive stress responsible for soil loss (Tavares and Amiotte-Suchet, 2007; Sanchez-Moreno et al., 2014) and rapid destruction of the island relief (Menendez et al., 2008; Llanes et al., 2009; Ramalho et al., 2013). The orography of Santiago Island, in particular, is characterized by its relatively high mountains (up to 1392 m in elevation), of enhanced rainfall. However, contrary to the other high elevation islands of the Cape Verde Archipelago with juvenile volcanic relief, Santiago presents dense and deeply incised erosional landforms (Ramalho, 2011). The SW side of the Island and Assomada region, which were rejuvenated by younger post-erosional volcanism, are local exceptions.

Topmost soil samples tend to be enriched in immobile elements when compared to average weathering profiles, providing an incomplete perspective of the nature of the regolith (Nesbit and Markoviks, 1997). On the other hand, bedload stream sediments are enriched in mobile elements when compared to the suspended load (Louvat and Allègre, 1998; Rad et al., 2006) and the soils in the source area (Rad et al., 2006). Despite the expected differences between topsoils and bedload deposits, an analysis of some geochemical parameters, such as weathering intensity and immobile element ratios, may offer relevant information on the spatial distribution of sediment generation processes. In the present research we systematically combine the geochemistry of six bedload stream samples of Santiago Island with the soils collected in their drainage areas (Fig. 1) in order to investigate: (1) compositional changes during sediment generation; and (2) spatial differences in weathering and erosion intensities, associating their variability with regions and geological units of the island. Particular attention is paid to the ways of interpreting data from the environmental geochemical atlas in the analysis of erosional processes and their spatial variability.

2. Geological and geomorphological setting

The Cape Verde Archipelago is a group of ten islands located 500 km west of Senegal's Cape Verde, on mainland Western Africa (Fig. 1A). The archipelago can be sub-divided into a northern chain (Santo Antão, São Vicente, Santa Luzia and São Nicolau islands) and an east-to-southern chain (Sal, Boavista, Maio, Santiago, Fogo and Brava). It is also possible to differentiate the eastern islands of Sal, Boavista and Maio from the remaining islands due to their lower and flat-lying relief, always below 450 m in elevation, and the predominance of an erosional landscape (Ramalho, 2011). In contrast, the western islands reach frequently 1000 m high and the constructional volcanic landforms are easily discerned. On Santiago and Santo Antão Islands the overall shield relief is still perceptible but the islands are deeply incised by stream valleys.

The Cape Verde Islands are genetically linked with hotspot volcanism (McNutt, 1988; Sleep, 1990) responsible for the Cape Verde Rise (Lancelot et al., 1978). This volcanic activity started in the

late Oligocene or Early Miocene, being probably older on Sal and Boavista islands (Holm et al., 2008; Ramalho et al., 2010a; 2010b). Geological mapping published by Serralheiro (1976) and the subsequent work of Matos Alves et al. (1979) allowed the establishment of the volcano-stratigraphy of Santiago Island, which comprises, from the oldest to the youngest, the following main geological units: Ancient Eruptive Complex, Flamengos Formation, Orgãos Formation, Pico da Antónia Eruptive Complex, Assomada Formation, Monte das Vacas Formation and Quaternary sediments. It is possible to identify periods of intense volcanic activity responsible for the growth of the island alternating with periods of longer-term volcanic quiescence when erosion and sedimentation were the dominant processes. The eruptive units can be organized into basement, shield-building and post-erosional units according to their development within the island's geological history framework (Holm et al., 2008; Ramalho et al., 2010a; 2010b).

The Ancient Eruptive Complex constitutes the basement unit of Santiago Island. Its outcrops are scattered throughout the island, occurring in the valleys where erosion has worn away the most recent geological units (Fig. 1B). The largest outcrops occur in the southern and central regions of the island. This unit is mostly a dyke complex with volcanic plugs and intra-volcanic breccias of diverse composition, including basanitic, basaltic, phonolitic and carbonatic (Matos Alves et al., 1979). In general, the rocks of the Ancient Eruptive Complex are strongly fractured and altered. Several authors suggest that fragments of sea-floor basalts (MORB-type) occur within the Ancient Eruptive Complex (Gerlach et al., 1988; Davies et al., 1989), which may indicate an early submarine building with uplifted seafloor (Holm et al., 2008).

The Flamengos Formation and Pico da Antónia Complex constitute the shield-building units on Santiago Island. These units are separated by the sedimentary rocks of the Orgãos Formation. The Flamengos Formation occurs essentially in the centre and south of Santiago Island, with the widest outcrops being located on the northeast-facing side of the island. It is formed by a succession of pillow-lavas with subordinated breccias and tuffs. The Pico da Antónia Complex is the most extensive outcropping unit of Santiago Island, corresponding to the main shield-building stage. This complex is essentially formed by thick sequences of subaerial and submarine lava flows intercalated with pyroclastic rocks. Some authors consider that the unit is composed of a lower member that seems to be exclusively submarine and an upper member mainly with subaerial volcanic rocks (Martins et al., 2008; Ramalho et al., 2010b).

The Assomada and Monte das Vacas formations correspond to the post-erosional units of Santiago Island. Serralheiro (1976) considered that the Assomada Formation is older than the Monte das Vacas Formations, but later radiometric data suggest that they are coeval (Holm et al., 2008). The Assomada Formation occupies a large depression between the two largest elevations of the island, Pico da Antónia (1392 m) and Serra da Malagueta (1063 m). It is constituted by basaltic lava flows and pyroclastes, originated exclusively from sub-aerial activity. The Monte das Vacas Formation is represented by 50 cinder cones of basaltic pyroclastic rocks and associated lava sequences (Johnson et al., 2012). Its constituting rocks are loosely aggregated and are exploited for construction materials, originating gullies and landslides on the flanks of the volcanic cones.

3. Materials and methods

The soil and bedload samples database came from the environmental geochemical atlas of Santiago compiled by Cabral Pinto (2010) for Santiago Island. For each sampling site, composite samples (~1 kg), made up of five grabs, were collected over an area

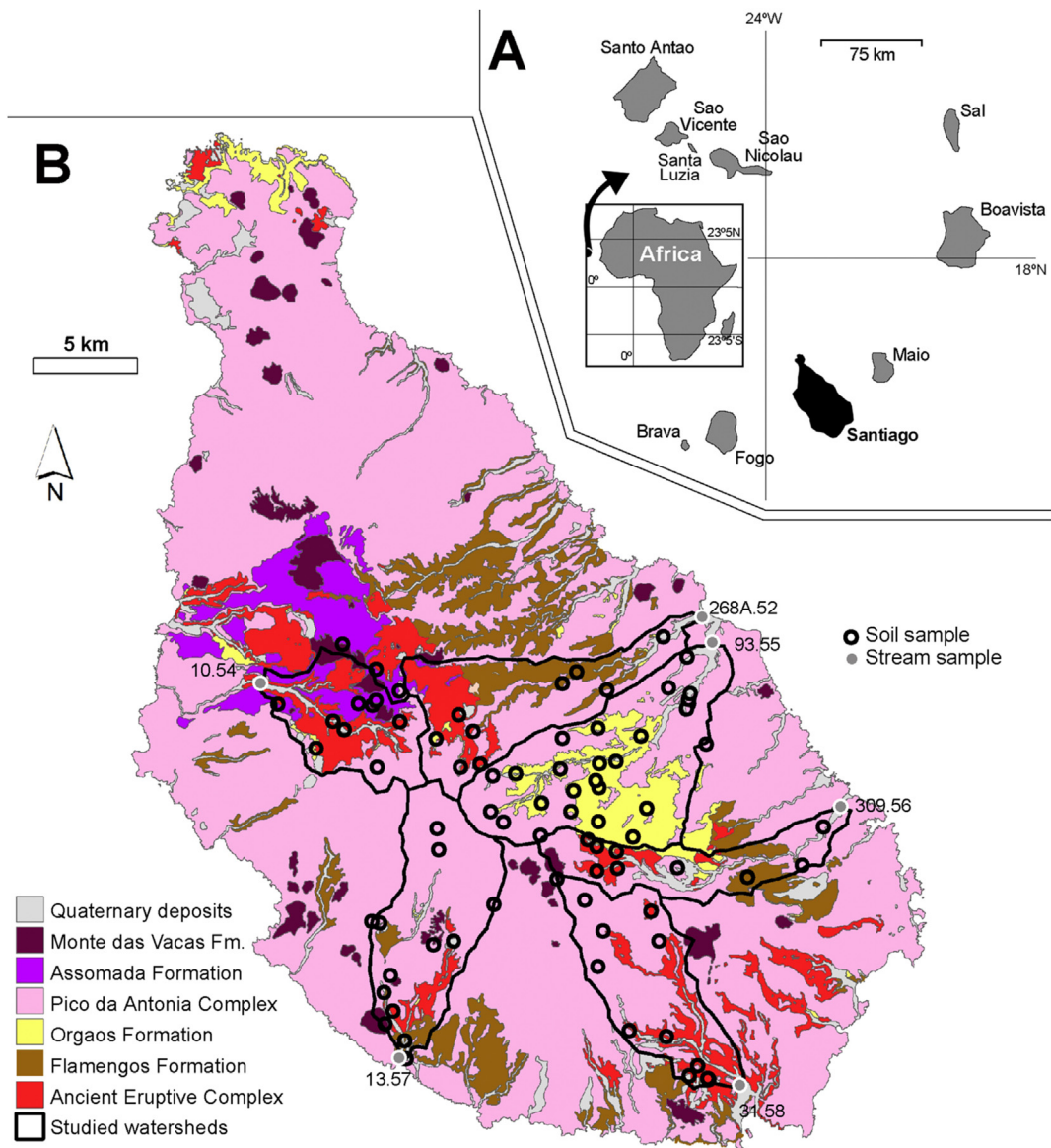


Fig. 1. Geological setting of Santiago Island. (A) Location of Santiago Island in the Cape Verde Archipelago and the western Africa shore. (B) Geological map of Santiago Island (modified from Serralheiro, 1976) and location of the soil and bedload sediment samples.

of about 100 m². As the sampling sites were selected to represent pristine soils and bedload stream sediments, locations near factories or roads with heavy traffic and arable soils were avoided. The samples were dried at 35–40 °C, sieved to <2 mm through a plastic sieve, homogenized and quartered. Sub-samples of 50 g each were obtained and crushed to <75 µm for analysis. The chemical analyses were performed in the ACME Analytical Laboratories, Ltd (Vancouver, Canada). Each sample was digested in *aqua regia* and analysed by inductively coupled plasma-mass spectrometry (ICP-MS). Although there is a risk that the digestion with *aqua regia* did not destroy all silicates (Darnley et al., 1995), this method is commonly used in environmental studies and the pattern of distribution of *aqua regia* results for many non-mobile elements resemble those obtained with total digestion (Ren et al., 2015). The chemical results were subjected to several data quality tests in order to determine which elements have reliable data for analysis (Cabral Pinto et al., 2015). For this research 6 bedload stream sediments were selected (10.54, 13.57, 31.58, 93.55, 309.56 and 268A.52; Fig. 1) and the soils collected within their watersheds (105 samples). The

chemical elements selected for this research are: Al, Ba, Ca, Co, Cr, Cu, Fe, K, La, Mg, Mn, Na, Ni, P, Pb, Sc, Sr, Th, Ti, U, V and Zn. The delimitation of the catchment areas that drain to the stream sediment sampling points was performed using a Digital Elevation Model (DEM) based on a Shuttle Radar Topography Mission (SRTM) image with the package Arc Hydro (ArcGIS 10). This software package was also used to quantify the outcropping areas of the main geological units.

In order to calculate the average soil composition in each catchment area (ASC), a weighted average based on the composition of the soils samples collected in each catchment was calculated according to the following equation:

$$X_i = A_1 * X_{i1} + A_2 * X_{i2} \dots A_n * X_{in},$$

where X_i is the average concentration of element i in the topsoils of the catchment, A_1 to A_n are the spatial proportions of each lithologic unit (1 to n) within the watershed and X_{i1} to X_{in} are the average concentrations of element i in the topsoils of the each

lithologic. Soils collected within a 1 km buffer from the watershed were also considered.

4. Results and discussion

4.1. Composition of the stream sediments and topsoils in the respective catchments

The soil and bedload stream sediment geochemical dataset is shown in [Appendix A](#). Relative to the primitive mantle ([Palme and O'Neill, 2004](#)), all bedload and soil samples are depleted in Mg, Cr, and Ni and enriched in Sr, Ba, La, Th, U and Pb ([Fig. 2](#)). The strongest enrichments are found for Sr, La and Pb while Cr and Ni display the strongest depletions. Most soils and sediments are also enriched in Ti. The concentrations of Na, Ca, Mn, Al, Fe and P, as well as V, Cu and Zn, in the soils and sediment samples can be either higher or lower than in the primitive mantle. Soils formed on eruptive units display highly variable compositions, in particular when parented with the Ancient Eruptive and Pico da Antónia complexes, and there are no significant differences between the soils associated with distinct geological units ([Fig. 2](#) and [Table 1](#)). In spite of this variability, the topsoils associated with the Assomada Formation tend to yield higher Sr, Ba, Pb and P and lower K, Mg, Ti, V, Cr, Co, Ni and Cu than those associated with the Flamengos Formation.

Element concentrations in the soils collected in the sedimentary units (Orgãos Formation and Quaternary deposits) and the present-day bedload stream deposits fall within the range of values exhibited by the topsoils associated with the eruptive rocks ([Fig. 2](#)). However, if we consider only the most common soil compositions (between 1st and 3rd quartiles, [Fig. 2](#)), bedload sediments tend to be slightly enriched in Na, Mg, Ca and Sr and depleted in Sc, Th and U relative to soils. These compositional differences are particularly obvious when the fluvial sediments are compared with the soils

collected in the respective catchment areas ([Fig. 3](#); [Table 1](#)). When compared to the respective ASC, all bedload samples show a strong Na enrichment and usually moderate Ca and Mg enrichment. Significant depletions in Sc and, to a lesser extent, in Al, Ba, Th, P and U are also observed in most bedload stream sediments. Depending on the catchment, K, Pb, Ti, Cr and Ni concentrations can be either substantially higher or lower in the bedload sample than in the corresponding ASC ([Fig. 3](#)).

4.2. Weathering intensity and erosion

Weathering is the processes responsible for the degradation of rocks (either chemically or physically), forming loose materials that can be eroded. Hence, one can expect that higher erosive rates occur when weathering stages are more advanced. However, sectors where faster erosion of the regolith is occurring tend to yield compositional features indicative of lower weathering intensities ([Le Pera et al., 2001; Dinis et al., 2016](#)) and this relation is probably particularly evident in areas under strong denudation and with thin regolith profiles, such as the volcanic islands in semi-arid settings ([Menendez et al., 2008; Llanes et al., 2009; Ramalho et al., 2013](#)).

Several geochemical indices were applied to determine the extent of weathering ([Table 2](#)). The weathering intensity is classically assessed with the chemical index of alteration (CIA; [Nesbitt and Young, 1982](#)), which depicts the decomposition of feldspar with consequent increase in Al_2O_3 concentration along with CaO, Na₂O and K₂O depletion. However, in soils and sediments derived from basaltic rocks the evaluation of weathering intensity should also take into consideration the decomposition of Fe and Mg minerals. [Babechuk et al. \(2014\)](#) proposed a mafic index of alteration (MIA) that extends the CIA formulation by adding Fe and Mg contents. Two equations were defined, one for oxidising environments (MIA(O)) and one for reducing environments (MIA(R)), their differences being grounded on the different behaviour of Fe with redox conditions. We applied the equation for oxidising environments because these weathering conditions are the most common in present-day arid regions (e.g. [Chuchman and Lowe, 2011](#)). Studies of exogenous process in Cape Verde ([Marques et al., 2014a, 2014b, 2016](#)) and other volcanic islands ([Nelson et al., 2013; Goodfellow et al., 2013](#)) also demonstrate that oxidising environments are clearly prevalent in these settings.

The ternary diagram A-CN-K ([Nesbitt and Young, 1982](#)) can be used to graphically visualize the CIA index ([Fig. 4](#)). All samples are plotted close to the Al-Ca join, reflecting their relatively low K content. Except for a few soils formed over the Ancient Eruptive Complex and Flamengos Formation, soil samples tend to yield higher CIA than bedload samples. CIA values for rocks are lower than all but one of the stream samples. Likewise, the MIA index can be envisaged with the diagram AF-CNK-M ([Babechuk et al., 2014](#)). As with the A-CN-K, stream sediments tend to yield lower MIA than soils and higher MIA than non-weathered rocks. The highest CIA and MIA values are found in soils formed on the youngest eruptive units, the Pico da Antónia Complex and the Assomada/Monte das Vacas formations ([Fig. 4](#)). However, given the high range of MIA and CIA values yielded by the geological units, in particular in the Ancient Eruptive and Pico da Antónia complexes, the weathering indices for the soils must be significantly affected by the composition of the parent rocks.

Orographic rain in Santiago Island is responsible for wetter climates in inland locations with higher elevation when compared to the arid or semi-arid littoral zone ([Ferreira, 1987](#)). This climatic zonation is not reflected in the indices of weathering ([Fig. 5](#)). In fact, CIA and MIA do not show any relation to altitude ([Fig. 5](#)) and some of the topsoils with evidence of more advanced chemical alteration are located in low-altitude arid sectors. Most samples displaying

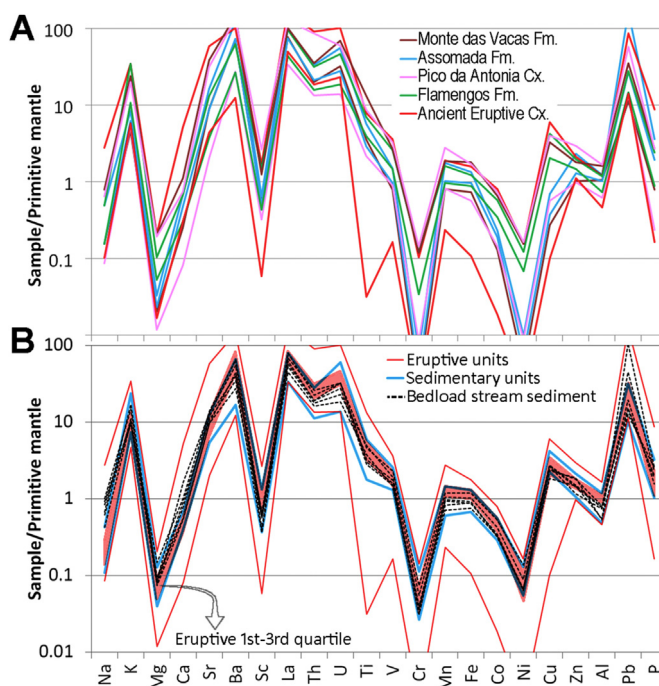


Fig. 2. Geochemical composition of topsoil and bedload deposits. (A) Range of values for eruptive units. (B) Bedload stream sediments, maximum and minimum values for soils collected in sedimentary and eruptive geological units and the 1st–3rd quartiles range of soils on eruptive rocks. Compositions are normalised to the primitive mantle (after [Palme and O'Neill, 2004](#)).

Table 1
Synthesis of soils and stream sediments compositional data.

		Al (%)	Ba (ppm)	Ca (%)	Co (ppm)	Cr (ppm)	Cu (ppm)	Fe (%)	K (%)	La (ppm)	Mg (%)	Mn (%)	Na (%)	Ni (ppm)	P (%)	Pb (ppm)	Sc (ppm)	Sr (ppm)	Th (ppm)	Ti (%)	U (ppm)	V (ppm)	Zn (ppm)
Soils in geological units																							
CC	Mean	2.57	216.67	1.02	37.57	130.47	58.83	5.61	0.36	33.00	2.00	0.09	0.08	124.07	0.17	3.80	6.73	153.00	2.70	0.42	0.43	150.33	76.33
	St.Dev	0.76	95.44	0.26	13.20	68.82	20.85	2.15	0.23	15.62	0.73	0.05	0.03	19.83	0.09	2.01	3.62	9.54	0.82	0.03	0.15	58.77	31.77
CB	Mean	3.79	220.76	1.07	44.16	126.32	70.06	6.30	0.32	37.04	1.94	0.10	0.05	142.91	0.14	3.25	9.81	166.08	3.52	0.47	0.62	161.88	76.40
	St.Dev	0.40	82.85	0.15	5.94	53.23	8.63	0.67	0.09	7.30	0.35	0.02	0.02	36.93	0.05	0.84	2.57	38.24	0.61	0.11	0.19	18.56	8.45
MV	Mean	5.48	824.57	1.01	44.60	91.30	40.43	8.52	0.27	62.43	2.18	0.15	0.08	131.37	0.14	4.69	10.09	309.86	5.24	0.99	1.04	141.43	81.14
	St.Dev	0.75	174.16	0.65	21.56	106.92	26.84	2.33	0.19	6.63	1.65	0.03	0.06	135.21	0.07	1.39	2.94	216.17	1.16	0.40	0.43	56.20	14.85
As	Mean	4.48	730.60	1.20	21.18	10.40	10.02	6.86	0.18	58.00	0.61	0.15	0.08	14.46	0.23	13.12	7.10	239.80	4.50	0.47	0.78	102.40	97.60
	St.Dev	0.31	148.10	0.20	1.44	2.88	2.95	1.04	0.03	6.63	0.09	0.03	0.04	3.09	0.06	11.01	0.60	64.20	0.91	0.14	0.25	20.28	23.28
PA	Mean	3.99	413.76	0.90	50.04	146.13	51.74	7.19	0.27	47.32	1.79	0.13	0.05	177.12	0.14	5.14	11.45	189.47	4.97	0.55	0.79	161.47	81.62
	St.Dev	0.76	162.89	0.35	13.75	80.37	16.25	1.67	0.09	13.34	0.96	0.04	0.03	75.95	0.06	2.20	5.12	117.68	2.39	0.17	0.27	49.61	19.95
Fl	Mean	3.78	321.25	1.10	46.68	147.91	63.09	6.82	0.51	44.88	1.66	0.12	0.09	150.79	0.14	3.81	9.84	187.13	4.04	0.68	0.80	169.63	92.63
	St.Dev	0.63	88.38	0.27	6.58	67.71	15.33	0.79	0.23	14.18	0.36	0.02	0.03	32.66	0.05	0.92	3.51	63.61	0.89	0.15	0.22	30.17	8.88
CA	Mean	3.66	385.86	1.61	48.08	146.85	69.72	7.12	0.34	53.91	1.60	0.14	0.08	133.11	0.17	5.63	12.47	220.27	5.18	0.37	0.90	188.36	88.55
	St.Dev	0.83	155.20	2.18	17.39	70.78	33.59	1.94	0.19	17.87	0.90	0.04	0.14	72.82	0.14	3.58	4.29	229.20	2.72	0.23	0.39	56.51	15.01
Stream sediment and respective catchment																							
10.54	ASC	3.72	520.16	1.88	34.41	85.93	34.96	6.44	0.20	54.97	1.42	0.12	0.07	99.58	0.23	6.17	9.22	291.12	4.60	0.43	0.75	145.46	72.62
	SS	2.19	235.00	1.91	32.10	90.00	36.80	5.56	0.26	43.00	1.85	0.09	0.24	120.70	0.22	2.30	4.30	217.00	3.40	0.36	0.60	129.00	78.00
13.57	ASC	4.70	546.32	1.06	51.01	146.80	58.71	8.00	0.28	62.41	1.84	0.14	0.06	164.31	0.15	5.93	14.61	252.35	6.05	0.61	0.92	185.14	88.07
	SS	3.22	437.00	2.13	53.60	185.40	48.10	7.39	0.24	54.00	3.27	0.12	0.22	254.30	0.17	2.60	7.40	283.00	4.00	0.59	0.70	195.00	96.00
31.58	ASC	3.60	436.92	0.83	49.99	158.29	47.27	8.08	0.35	48.60	1.55	0.15	0.05	167.98	0.14	5.32	11.46	132.20	4.63	0.49	0.84	188.29	82.81
	SS	2.12	370.00	3.45	33.80	79.00	46.40	5.76	0.44	47.00	1.93	0.10	0.17	118.60	0.22	19.40	4.90	267.00	4.70	0.41	0.70	149.00	100.00
309.56	ASC	3.81	302.63	0.90	49.73	166.78	64.24	6.55	0.36	39.45	1.75	0.13	0.05	158.44	0.13	4.87	11.10	179.00	4.48	0.49	0.76	159.63	88.10
	SS	3.11	299.50	1.27	43.00	139.15	55.05	6.38	0.29	36.00	2.11	0.11	0.18	164.05	0.16	2.80	6.75	197.00	3.15	0.63	0.50	164.50	79.50
268A.52	ASC	3.58	347.95	1.09	47.79	130.64	60.62	6.74	0.27	46.82	1.74	0.13	0.05	164.34	0.16	4.98	9.36	205.60	4.41	0.50	0.88	155.87	84.11
	SS	3.05	273.00	1.67	35.60	101.00	54.00	5.41	0.38	39.00	1.69	0.10	0.26	122.00	0.20	8.30	8.00	243.00	3.40	0.38	0.70	136.00	76.00
93.55	ASC	3.66	259.74	1.03	48.31	142.57	64.36	6.48	0.32	37.09	2.07	0.11	0.06	175.77	0.13	3.53	9.89	165.32	3.58	0.52	0.59	151.93	79.64
	SS	2.96	184.00	1.13	33.40	93.00	53.10	4.74	0.26	31.00	1.63	0.07	0.11	123.90	0.13	3.60	6.80	195.00	2.90	0.47	0.40	125.00	62.00

CC: Quaternary sedimentary units; CB: Orgâos Formation; MV: Monte das Vacas Formation; As: Assomada Formation; PA: Pico da Antónia Complex; Fl: Flamengos Formation; CA: Ancient Eruptive Complex; ASC: Average soil composition in the catchment area. SS: Stream sediment.

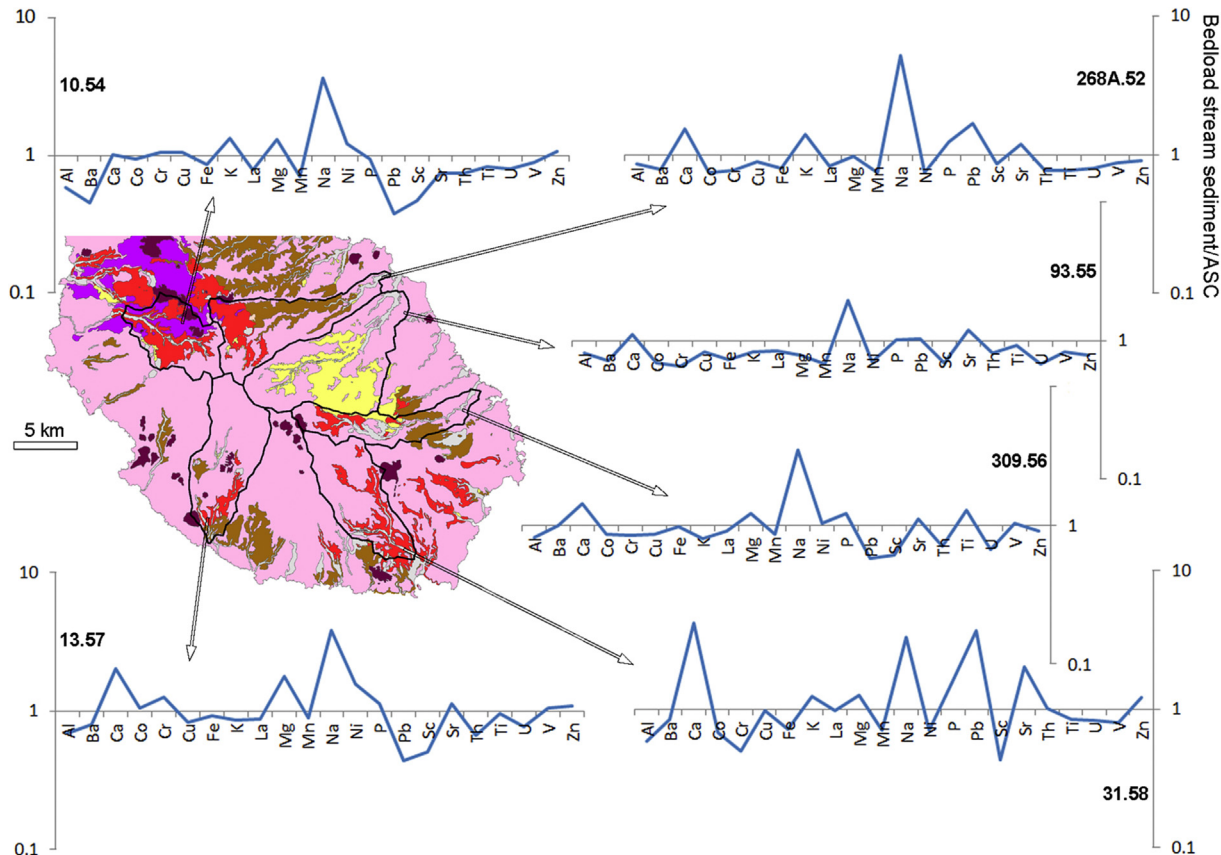


Fig. 3. Average soil composition (ASC; see text for explanation) of the studied catchments normalised to the corresponding bedload stream sediment.

Table 2

Weathering indices selected for this work.

Weathering index	Formula ^a	Reference	Limitations to the application in Santiago Island
CIA	$\text{Al}_2\text{O}_3/(\text{Al}_2\text{O}_3 + \text{K}_2\text{O} + \text{Na}_2\text{O} + \text{CaO})^{\text{a}}100$	Nesbitt and Young, 1982	Does not consider Fe-- and Mg-minerals; values for fresh rock composition are highly variable; carbonatites with very low values
MIA	$(\text{Al}_2\text{O}_3 + \text{Fe}_2\text{O}_3)/(\text{Al}_2\text{O}_3 + \text{K}_2\text{O} + \text{Na}_2\text{O} + \text{CaO} + \text{Fe}_2\text{O}_{3(t)} + \text{MgO})^{\text{a}}100$	Babechuk et al., 2014	Values for fresh rock composition are highly variable; carbonatites with very low values
MIA-x	$(\text{Al}_2\text{O}_3 + \text{Fe}_2\text{O}_{3(t)})/(\text{Al}_2\text{O}_3 + \text{K}_2\text{O} + \text{Na}_2\text{O} + \text{Fe}_2\text{O}_{3(t)} + \text{MgO})^{\text{a}}100$		Difference between carbonatites and the remaining rocks is minor, but the overall variability for fresh rocks is very high

^a In molar proportions.

strong weathering (CIA>80; MIA>70) were collected in catchments of the SW flanking side of Santiago Island (Fig. 5), which could be attributed to a parent-rock control on composition or indicate that the slopes on drier leeward side of the island tend to be less affected by erosion. The bedload stream sediments from the eastern side of Santiago Island (represented by 268A.52, 93.55 and 309.56) yield CIA and MIA values not substantially different from the ASC (Fig. 6). The resemblance of the bedload deposits to ASC suggests that the sediment was mostly derived from homogenously shallow weathering profiles. The possibility of an association with shallow regolith is also supported by the relatively low MIA values of ASC when compared to the remaining catchments (Fig. 6) and is compatible with the wider east-facing areas in the region with higher rainfall (Ferreira, 1987) and risk of erosion (Tavares and Amiotte-Suchet, 2007). Major differences in weathering proxies between the bedload samples and the catchment's average soil are found for the river that drains southward and westward (represented by 31.58, 13.54 and 10.54). Raised volumes of sediment

generation in restricted locations, including poorly weathered rock fragments, justifies the MIA and CIA values very close to the fresh rocks in some bedload deposits (Figs. 5 and 6).

The occurrence of carbonatites in Santiago Island (Serralheiro, 1976; Silva et al., 1981) and consequent non-silicate bound CaO brings supplementary difficulties to the application of these indices. A few soil samples associated with carbonatites of the Ancient Eruptive Complex are plotted very close to the CN vertex of the A-CN-K diagram and to the CNK-M join of the AF-CN-K-M diagram due to their high Ca (and Mg) concentrations (Fig. 4). To ensure that the weathering intensities are not biased by the presence of carbonate and phosphate minerals, a modified version of the MIA index which does not take CaO content into consideration (MIA-x) is also used. Similar approaches were already adopted for CIA index in sediments with diagenetic carbonate or derived from carbonate sedimentary rocks (Garzanti et al., 2014; Dinis et al., 2016). As with CIA and MIA, high MIA-x values are found for topsoils in the catchments of west- and south-draining streams (Figs. 5

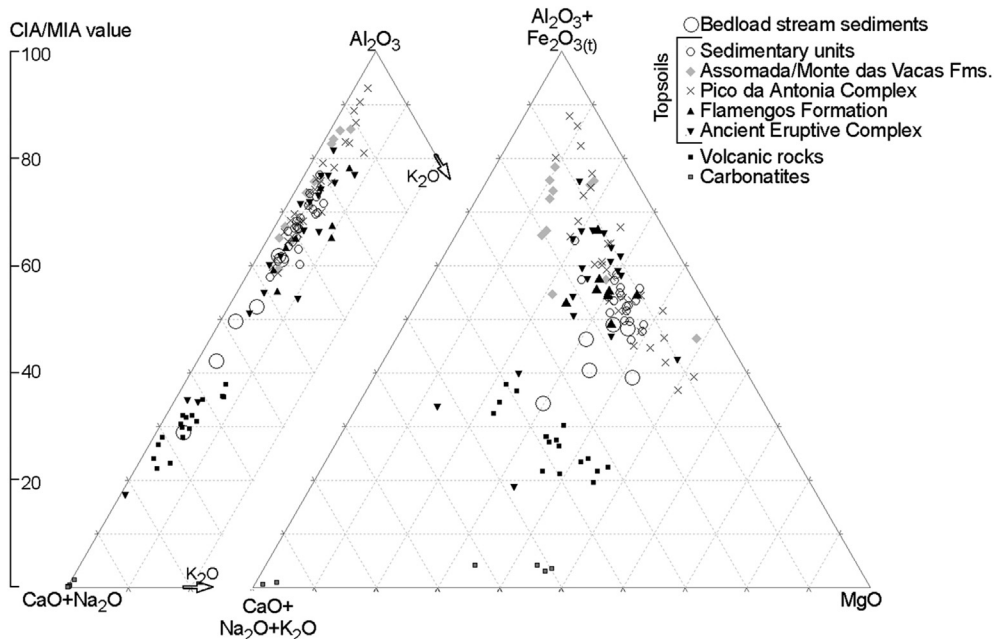


Fig. 4. Ternary diagrams $\text{Al}-\text{Ca} + \text{NaK}$ and $\text{Al} + \text{Fe}-\text{Ca} + \text{Na} + \text{K}-\text{Mg}$. CIA (Nesbitt and Young, 1982) and MIA (Babechuk et al., 2014) weathering indices are also indicated. Composition of carbonatites from Hoernle et al. (2002); Santiago Island volcanic rocks from Doucelance et al. (2003) and Martins et al. (2010).

and 6).

4.3. Sediment sources

When compared to the ASC, bedload sediment samples show lower values of weathering intensity and depletion in several elements that tend to be non-mobile, such as Al, Fe, La, Mn, Sc, Th and, except for one catchment, Ti (Fig. 3). Moderate depletion in the stream sediments is also observed for Ba and U. Although Ba tends to be soluble (e.g. Buggle et al., 2011), its mobility in weathering profiles is lower than K (Bouchez et al., 2011; Garzanti et al., 2013; Garzanti and Resentini, 2016) and significant enrichment in basalt-parented regolith can occur (Eggerton et al., 1987; Price et al., 1991). However, due to the low U concentrations in basaltic rocks when compared to average world dust, abnormal abundance in soils from volcanic islands has been associated with dust deposition (Pett-Ridge et al., 2007) and this possibility is particularly plausible in regions like Santiago Island that fall within the Sahara-Sahel dust corridor (Goudie and Middleton, 2001; Prospero et al., 2002; Dunion and Velden, 2004; Zhang and Pennington, 2004). Local input of some elements due to human activities can also be considered. For example, the highly variable Pb and P contents may be partially related to human activities. In conclusion, bedload deposits represent an intermediate composition between two endmembers: the non-weathered rock (which tends to be enriched in mobile elements) and the more weathered topsoil (which tends to be enriched in non-mobile elements and may incorporate allochthonous material associated with the deposition of atmospheric dust or introduced by human activities). The proportion of the two endmembers in a given bedload deposit should reflect the spatial distribution of weathering and erosion processes in the catchment area.

As weathering state is expected to influence the concentration of both mobile elements and non-mobile elements, an analysis of the nature of the source units based on soils and sediment compositions must consider a combination of non-mobile elements. Ternary plots La-Co-Cr and La-Th-Ti were selected for this

provenance analysis because the elements involved do not show major differences in bedload concentration relative to ASC (Fig. 3). These ternary plots isolate several soil samples from the bedload samples and the remaining soils of the respective catchment (Fig. 7). The immobile elements that are either enriched or depleted in the bedload samples with respect to the corresponding catchment ASC, such as Co and Cr (Fig. 3), can also be applied to identify source areas that are supplying anomalously high or low sediment yields. Soils of Santiago Island with higher Cr and Co abundances tend to be associated with mafic volcanic rocks (Marques et al., 2012; Cabral Pinto et al., 2015) and the enrichment in these elements in bedload stream sediments relative to the ASC (samples 10.54 and 13.57; Fig. 3) points to increased supply from mafic-derived soils (Fig. 7). Hence, soil samples belonging to the catchment areas of samples 10.54 and 13.57 that are isolated in the La-Co-Cr and La-Th-Ti plots (Fig. 7) probably came from sectors that have contributed low volumes of sediment. The relatively high CIA, MIA and MIA-x weathering indices yielded by most of these soil samples (Fig. 5) reinforce the hypothesis that they correspond to locations protected from erosional processes. The majority of these soil samples are parented with the Assomada Formation. In contrast, "uncharacteristic" La-rich and Ti-poor samples collected in the catchment area of 31.58 probably have correspondence with sectors strongly affected by erosion, explaining the differences between the ASC and bedload sediment compositions (Fig. 7).

4.4. Implications for the interpretation of Santiago Island denudation

The topsoil and bedload stream samples can also be applied in the interpretation of the longer-term denudation. Non-weathered lava surfaces have a crucial role in the protection from coastal and fluvial erosion (Ramalho et al., 2013). The advanced weathering of the shield building units may have promoted local failure of the protection to erosion, being the more elevated areas of the island, where rainfall erosivity is high (Sanchez-Moreno et al., 2014) and climatic conditions favour weathering progress, particularly

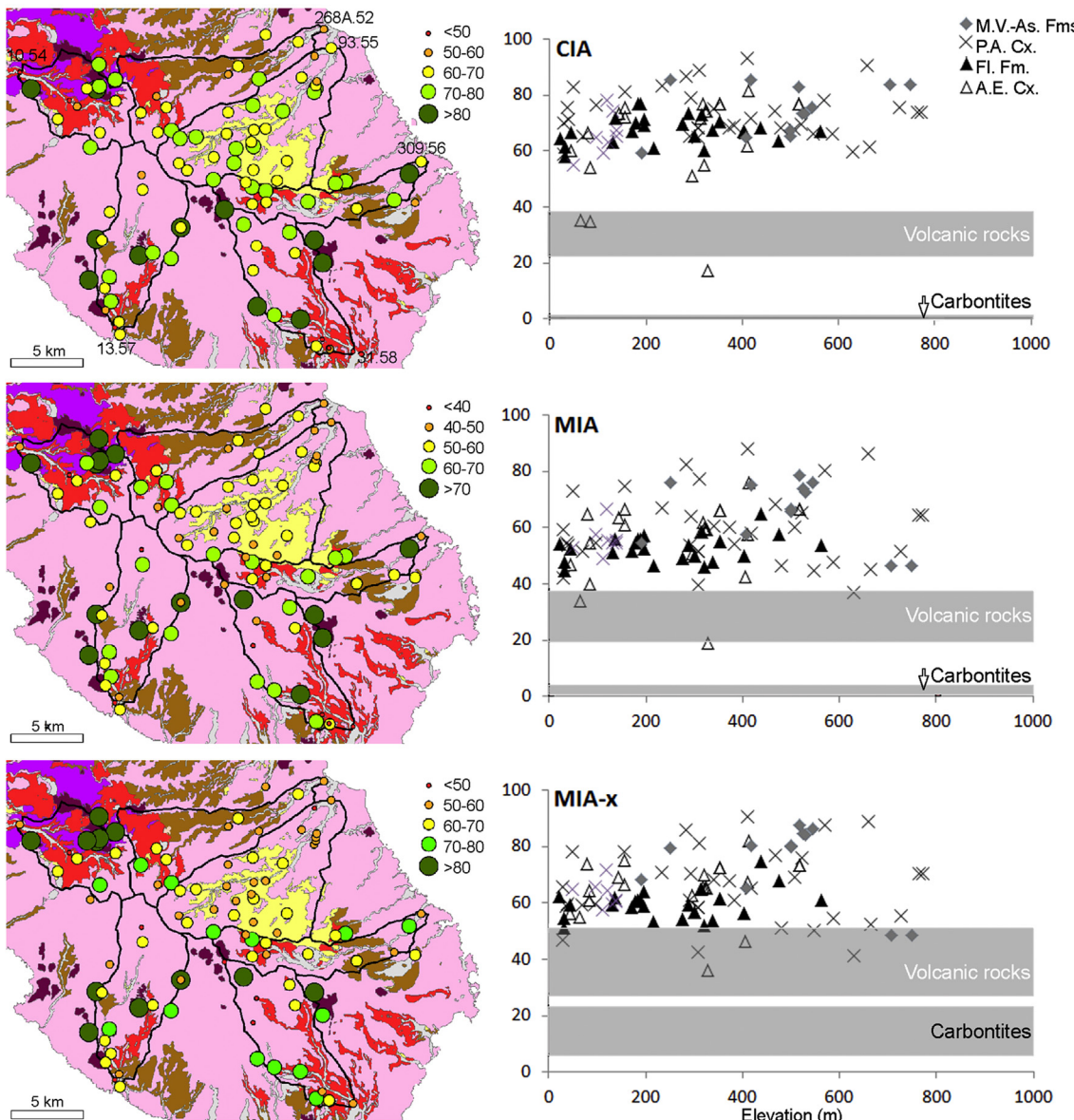


Fig. 5. Values of CIA (Nesbitt and Young, 1982), MIA (Babechuk et al., 2014) and the modified version of MIA without Cao (MIA-x; see text for explanation) weathering indices for bedload samples with location in Santiago Island. Santiago Island carbonatites (from Hoernle et al., 2002) and volcanics rocks (from Doucelance et al., 2003; Martins et al., 2010) are represented for comparison. M.V.-As. Fms.: Monte das Vacas-Assomada formations; P.A. Cx.: Pico da Antónia Complex; Fl. Fm.: Flamengos Formation; A.E. Cx.: Ancient Eruptive Complex. Key for geological map in Fig. 1.

affected by the erosional processes. The exhumation of large outcrops of the Ancient Eruptive Complex in relatively high elevations (ca. 200–650 m) at the centre of the island reflects the advance of Santiago Island's denudation.

The asymmetry between the SW- and NE-facing sides of Santiago Island is partially attributed to different stages of the denudation process. Although the geomorphic evolution of oceanic islands largely depends on the degree of development of drainage networks, the morphology of the drier leeward flank of the island (i.e., the SW side that is less affected by erosion) seems to reflect the younger post-erosional rejuvenation of the landscape by extensive lava shields of the Assomada and Monte das Vacas formations (Johnson et al., 2012). In the NE-facing side of the island, the capping rocks of the Pico da Antónia Complex are deeply incised by numerous streams that exhumed the Órgãos and Flamengos formations and can reach the Ancient Eruptive Complex. Bedload

stream sediments in this part of the island (represented by 268A.52, 93.55 and 309.56) are mainly sourced by the weathering profiles, with a minor contribution of poorly-weathered rocks, explaining the similarities between bedload deposits and ASC compositions (Figs. 3, 6 and 7).

The rocks of the Pico da Antónia Complex still constitute an effective barrier to the progress of erosion in places of low elevation where weathering and rainfall are less intense, namely in the case of the rivers with south drainage (represented by samples 31.58 and 13.57). Where the fluvial incision reaches the highly altered Ancient Eruptive Complex it is expected that it will progress swiftly upstream, promoting the island's denudation. Rapid dismantling of this unit justifies the very low values of MIA and CIA in the bedload samples, in particular in 31.58 (Fig. 6). The Assomada Formation in a west-draining stream (represented by 10.54) constitutes a younger erosion-resistant cap formed during the post-erosional volcanic

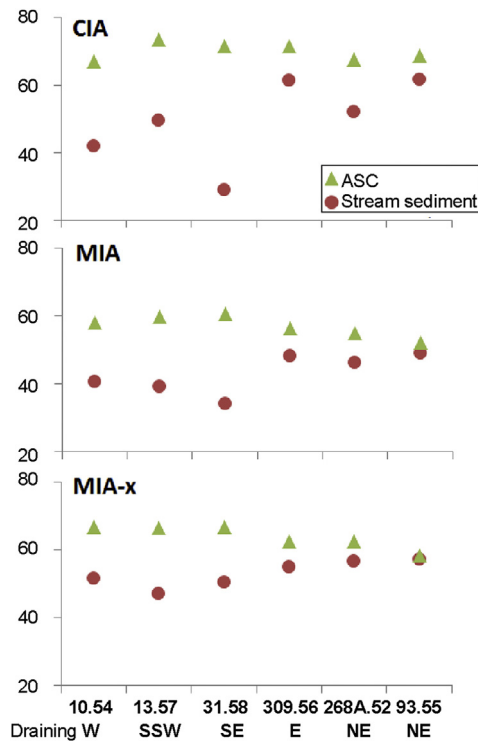


Fig. 6. Comparison of CIA, MIA and MIA-x weathering intensities in bedload deposits with the catchment's average soil composition (ASC).

phase, as demonstrated by the ratios of non-mobile elements (Fig. 7) and the weathering intensity indices in topsoil samples (Fig. 5), which indicate that minor amounts of detritus are supplied by the regolith sequences that rest on this geological unit. The presence of preserved plateaus in the southern and western sides of the island, contrasting with the more dissected NE side (Marques, 1990), reinforces this possibility. Regardless of its nature, when post-erosional volcanic landscape rejuvenation is more extensive, bedload stream deposits should include a significant proportion of poorly-weathered rocks. Under these conditions, the composition of the topsoils is more variable and major differences between bedload stream deposits and the topsoils in the catchment areas are expected.

5. Conclusions

The composition of bedload stream deposits is somewhere between that of the fresh rocks (usually enriched in mobile elements) and the topsoils (usually enriched in non-mobile elements) of their drainage areas and may be either closer to non-weathered rocks or to the surface soils. This fact raises a fundamental difficulty in the application of the composition of surface soils and bedload deposits in the analysis of differential detritus supply from distinct regions within a catchment. The geochemical atlases of surface soils and bedload stream sediments provide valuable information about the weathering/erosion processes at the catchment scale and their spatial variability, despite not being designed for these purposes and not routinely account for the numerous factors that control

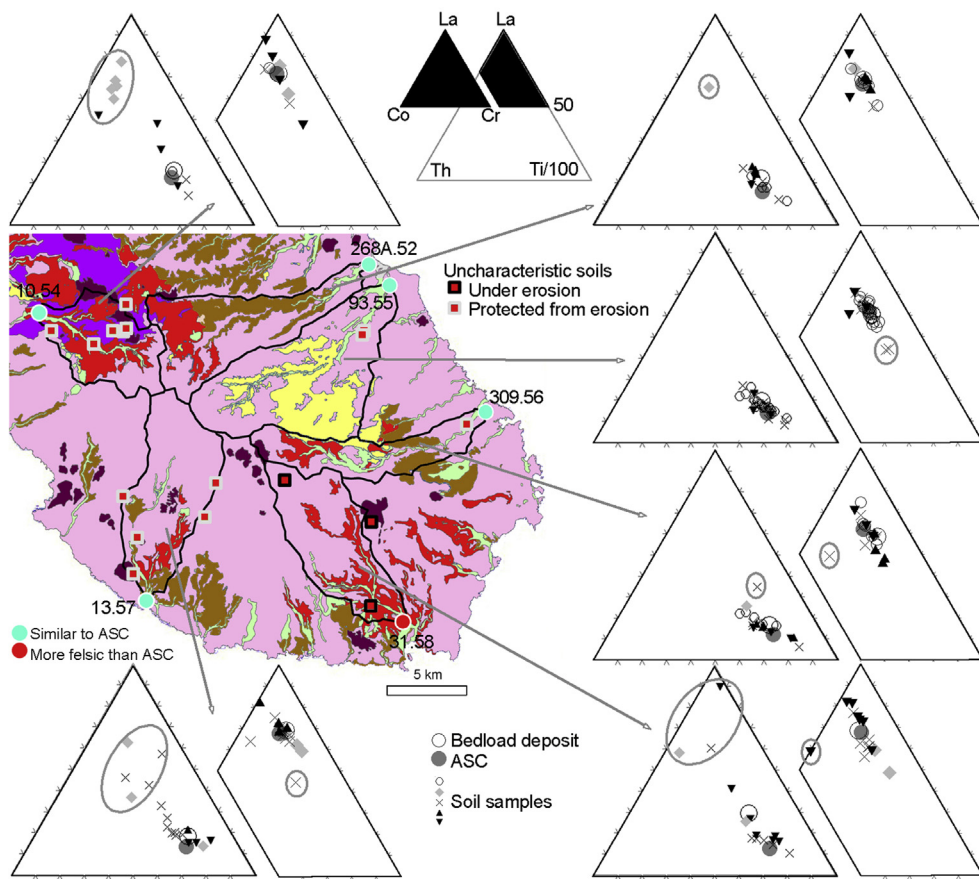


Fig. 7. Ternary diagrams La–Co–Cr and La–Th–Ti for the samples collected in each catchment and corresponding bedload deposit. Geological map and samples symbols keys in Fig. 1 and 4, respectively.

sediment composition (e.g., sorting processes, mineral breakdown, transformation during transitory deposition, etc.).

Where the average topsoil compositions are substantially different from bedload deposits and the variability of topsoil weathering intensity is high, bedload deposits should incorporate significant amounts of poorly-weathered rocks fragments. In these cases the erosion within the drainage basin is expected to vary spatially, with highly vulnerable and erosion-protected sectors. Ratios of non-mobile elements for the soils of the drainage basin help to identify the geological units and areas where erosion in the catchment is lower/higher. In contrast, a more similar composition of surface soils and bedload sediments, both with lower weathering intensities, suggests more widespread and homogeneously distributed erosion. This approach based on geochemical maps of topsoil and bedload stream sediments revealed that the NE- and S-to SW-facing flanks of Santiago Island are differently affected by weathering and erosion processes. The denudation is presently more advanced and widespread in the NE-facing side, whereas the SW side include extensive areas where protection from erosion is ensured by basaltic lava shields.

Acknowledgements

This study was supported by the FCT (Portuguese National Board of Scientific Research) grant SFRH/BPD/71030/2010, the Strategic Programs Geobiotec (UID/GEO/04035/2013), MARE (Marine and Environmental Sciences Centre) (UID/MAR/04292/2013), CNC (PEst-C/SAU/LA0001/2013) and CEMUC (UID/EMS/00285/2013). António Oliveira Cruz, Jorge Brito and Luís Filipe Tavares are acknowledged for the logistic support provided in Santiago Island by the Jean Piaget University of Cape Verde. We also appreciate the support given by the National Institute of Agricultural Research and Development of Cape Verde. MCP acknowledges with great affection the help of Ricardo Ramos during the field work. The manuscript benefited from careful and constructive reviews by M. Isabel Prudêncio and Ricardo S. Ramalho.

Appendix A. Supplementary data

Supplementary data related to this article can be found at <http://dx.doi.org/10.1016/j.apgeochem.2016.10.019>.

References

- Albanese, S., De Vivo, B., Lima, A., Cicchella, D., 2007. Geochemical background and baseline values of toxic elements in stream sediments of Campania region (Italy). *J. Geochem. Explor.* 93, 21–34.
- Arribas, J., Tortosa, A., 2003. Detrital modes in sedimenticlastic sands from low-order streams in the Iberian Range, Spain: the potential for sand generation by different sedimentary rocks. *Sediment. Geol.* 159, 275–303.
- Babechuk, M.G., Widdowson, M., Kamber, B.S., 2014. Quantifying chemical weathering intensity and trace element release from two contrasting basalt profiles, Deccan Traps, India. *Chem. Geol.* 363, 56–75.
- Bouchez, J., Lupker, M., Gaillardet, J., France-Lanord, C., Maurice, L., 2011. How important is it to integrate riverine suspended sediment chemical composition with depth? Clues from Amazon River depth-profiles. *Geochim. Cosmochim. Acta* 75, 6955–6970.
- Buggle, B., Glaser, B., Hambach, U., Gerasimenko, N., Markovic, S., 2011. An evaluation of geochemical weathering indices in loess-paleosol studies. *Quat. Int.* 240, 12–21.
- Cabral Pinto, M.M.S., Ferreira da Silva, E., Silva, M.M.V.G., Melo-Gonçalves, P., Candeias, C., 2014. Environmental risk assessment based on high-resolution spatial maps of potential toxic elements sampled on stream sediments of Santiago, Cape Verde. *Geosciences* 4, 297–315.
- Cabral Pinto, M.M.S., 2010. Cartografia Geoquímica da Ilha de Santiago com uma densidade de amostragem média/baixa. University of Aveiro (PhD thesis).
- Cabral Pinto, M.M.S., Ferreira da Silva, E.A., Silva, M.M.V.G., Melo-Gonçalves, P., Hernandez, R., Marinho, A.P., Inácio, M., Rocha, F., 2012. Mapping of estimated geochemical background values of some harmful metals in soils of Santiago island (Cape Verde archipelago). In: Nriagu, J., Szefer, P., Pacyna, J., Markert, B., Wünschmann, S. (Eds.), *Progress on Heavy Metals in the Environment*, pp. 101–122.
- Cabral Pinto, M.M.S., Silva, E.F., Silva, M.M.V.G., Melo-Gonçalves, P., 2015. Heavy metals of Santiago Island (Cape Verde) top soils: estimated Background Value maps and environmental risk assessment. *J. Afr. Earth Sci.* 101, 162–176.
- Cheng, T., Liu, X.M., Zhu, M.Z., Zhao, K.L., Wu, J.J., Xu, J.M., Huang, P.M., 2008. Identification of trace element sources and associated risk assessment in vegetable soils of the urban–rural transitional area of Hangzhou, China. *Environ. Pollut.* 151, 67–78.
- Chuchman, G.J., Lowe, D.J., 2011. Alteration, formation and occurrence of minerals in soils. In: Huang, P.M., Li, Y., Summer, M.E. (Eds.), *Handbook of Soil Sciences, Properties and Processes*. CRC Press, pp. 20.1–20.72.
- Darnley, A.G., Björklund, A., Bølviken, B., Gustavsson, N., Koval, P.V., Plant, J.A., Steenfelt, A., Tauchid, M., Xie, X., 1995. A Global Geochemical Database for Environmental and Resource Management. Recommendations for International Geochemical Mapping. Final Report of IGGP Project. UNESCO Publishing, p. 259.
- Davies, G., Norry, M., Gerlach, D., Cliff, R., 1989. A combined chemical and Pb–Sr–Nd isotope study of the Azores and Cape Verde hot spots; the geodynamic implications. *Geol. Soc. Lond. Special Publ.* 42, 231–255.
- de Caritat, P., Cooper, M., 2011. The national geochemical survey of Australia. *Geochim. atlas Austral.* 20, 1–557.
- Dinis, P.A., Dinis, J.L., Mendes, M.M., Rey, J., Pais, J., 2016. Geochemistry and mineralogy of the Lower Cretaceous of the Lusitanian Basin (western Portugal): deciphering palaeoclimates from weathering indices and integrated vegetational data. *Comptes Rendus Geosci.* 348, 139–149.
- Doucet, R., Escrig, S., Moreira, M., Gariépy, C., Kurz, M.D., 2003. Pb–Sr–He isotope and trace element geochemistry of the Cape Verde Archipelago. *Geochim. Cosmochim. Acta* 67, 3717–3733.
- Dunion, J.P., Velden, C.S., 2004. The impact of the Saharan Air Layer on Atlantic tropical cyclone activity. *Bull. Amer. Meteor. Soc.* 85, 353–365.
- Eggleton, R.A., Foudouli, C., Varkevisse, D., 1987. Weathering of basalt: changes in rock chemistry and mineralogy. *Clays Clay Minerals* 35, 161–169.
- Ferreira, D.B., 1987. La crise climatique actuelle dans l'archipel du Cap Vert. Quelques aspects du problème dans l'île de Santiago". *Finisterra XXII* (43), 113–152.
- Garzanti, E., Padoan, M., Setti, M., Peruta, L., Najman, Y., Villa, I.M., 2013. Weathering geochemistry and Sr–Nd isotope fingerprinting of equatorial upper Nile and Congo muds. *Geochem. Geophys. Geosyst.* 14, 292–316.
- Garzanti, E., Vermeesch, P., Padoan, M., Resentini, A., Vezzoli, G., Andò, S., 2014. Provenance of passive-margin sand (southern Africa). *J. Geol.* 122, 17–42.
- Garzanti, E., Resentini, A., 2016. Provenance control on chemical indices of weathering (Taiwan river sands). *Sediment. Geol.* 336, 81–95.
- Gerlach, D., Cliff, R., Davies, G., Norry, M., Hodgson, N., 1988. Magma sources of the Cape Verde Archipelago: isotopic and trace element constraints. *Geochimica Cosmochimica Acta* 52, 2979–2992.
- Goudie, A.S., Middleton, N.J., 2001. Saharan dust storms: nature and consequences. *Earth-Science Rev.* 56, 179–204.
- Goodfellow, B.W., Hillyer, G.E., Chadwick, O.A., 2013. Depth and character of rock weathering across basalt-hosted climosequences on Hawaii and Kauai. *Earth Surf. Process. Landforms* 39, 381–398.
- Hoernle, K., Tilton, G., le Bas, M.J., Duggen, S., Garbe-Shonberg, D., 2002. Geochemistry of oceanic carbonates compared with continental carbonatites: mantle recycling of oceanic crustal carbonate. *Contrib. Mineral. Pet.* 142, 520–542.
- Holm, P., Grandvoinet, T., Friis, J., Wilson, J.R., Barker, A.K., Plesner, S., 2008. An 40Ar–39Ar study of the Cape Verde hot spot: temporal evolution in a semi-stationary plate environment. *J. Geophys. Res. (Solid Earth)* 113 (B8), B08201.
- Inácio, M., Pereira, V., Pinto, M., 2008. The soil geochemical atlas of Portugal: overview and applications. *J. Geochem. Explor.* 98, 22–33.
- Ingersoll, R.V., 1990. Actualistic sandstone petrofacies: discriminating modern and ancient source rocks. *Geology* 18, 733–736.
- Johnson, M.E., Baarli, B.G., Cachão, M., da Silva, C.M., Ledesma-Vázquez, J., Mayoral, E.J., Ramalho, R., Santos, A., 2012. Rhodoliths, uniformitarianism, and Darwin: pleistocene and recent carbonate deposits in the Cape Verde and Canary archipelagos. *Palaeogeography, Palaeoclimatology, Palaeoecology* 329, 83–100.
- Johnsson, M.J., 1993. The system controlling the composition of clastic sediments. In: Johnsson, M.J., Basu, A. (Eds.), *Processes Controlling the Composition of Clastic Sediments*. Geol. Soc. America Spec. Paper, vol. 284, pp. 1–19.
- Komatina, M.M., 2004. *Medical Geology – Effects of Geological Environments on Human Health*. Elsevier Science and Technology, London.
- Le Pera, E., Arribas, J., Critelli, S., Tortosa, A., 2001. The effects of source rocks and chemical weathering on the petrogenesis of siliciclastic sand from the Neto River (Calabria, Italy): implications for provenance studies. *Sedimentology* 48, 357–378.
- Lancelot, Y., Seibold, E., Cepek, P., Dean, W., Eremeev, V., Gardner, J., Jansa, L., Johnson, D., Krasheninnikov, V., Pflaumann, U., Rankin, J.G., Trabant, P., Bukry, D., 1978. Site 368: Cape Verde Rise. In: Lancelot, Y., Seibold, E., Cepek, P., Dean, W., Eremeev, V., Gardner, J., Jansa, L., Johnson, D., Krasheninnikov, V., Pflaumann, U., Rankin, J.G., Trabant, P., Bukry, D. (Eds.), *Initial Rep. Deep Sea Drill. Proj.*, vol. 41. U.S. Government Printing Office, Washington, pp. 233–326.
- Llanes, P., Herrera, R., Gómez, M., Muñoz, A., Acosta, J., Uchupi, E., Smith, D., 2009. Geological evolution of the volcanic island La Gomera, Canary Islands, from analysis of its geomorphology. *Mar. Geol.* 264, 123–139.
- Levinson, A.A., 1974. *Introduction to Exploration Geochemistry*. Applied Publishing Ltd., Maywood.
- Lima, A., Albanese, S., Cicchella, D., 2005. Geochemical baselines for the

- radioelements K, U, and Th in the Campania region, Italy: a comparison of stream-sediment geochemistry and gamma-ray surveys. *Appl. Geochem.* 20, 611–625.
- Louvat, P., Allègre, C.J., 1997. Present denudation rates at Réunion island determined by river geochemistry: basalt weathering and mass budget between chemical and mechanical erosions. *Geochim. Cosmochim. Acta* 61, 3645–3669.
- Louvat, P., Allègre, C.J., 1998. Riverine erosion rates on São Miguel volcanic island, Azores archipelago. *Chem. Geol.* 148, 177–200.
- Marques, M.M., 1990. Caracterização das grandes unidades geomorfológicas da ilha de Santiago (República de Cabo Verde). Contribuição para o estudo da compartimentação da paisagem. *Garcia Orta* 17, 19–30.
- Marques, R., Prudêncio, M.I., Waerenborgh, J.C., Rocha, F., Dias, M.I., Ruiz, F., Ferreira da Silva, E., Abad, M., Muñoz, A.M., 2014a. Origin of reddening in a paleosol buried by lava flows in Fogo Island (Cape Verde). *J. Afr. Earth Sci.* 96, 60–70.
- Marques, R., Prudêncio, M.I., Rocha, F., Pinto, M.M.C., Silva, M.M.V., da Silva, E.F., 2012. REE and other trace and major elements in the topsoil layer of Santiago island, Cape Verde. *J. Afr. Earth Sci.* 64, 20–33.
- Marques, R., Prudêncio, M.I., Waerenborgh, J.C., Rocha, F., Ferreira da Silva, E., Dias, M.I., Madeira, J., Vieira, B.J.C., Marques, J.G., 2016. Geochemical fingerprints in topsoils of the volcanic Brava Island, Cape Verde. *Catena* 147, 522–535.
- Marques, R., Waerenborgh, J.C., Prudêncio, M.I., Dias, M.I., Rocha, F., Ferreira da Silva, E., 2014b. Iron speciation in volcanic topsoils from Fogo island (Cape Verde)—iron oxide nanoparticles and trace elements concentrations. *Catena* 113, 95–106.
- Martin, A.P., Turnbull, R.E., Rattenbury, M.S., Cohen, D.R., Hoogewerff, J., Rogers, K.M., Baisden, W.T., Christie, A.B., 2016. The regional geochemical baseline soil survey of southern New Zealand: design and initial interpretation. *J. Geochem. Explor.* 167, 70–82.
- Martins, S., Mata, J., Munhá, J., Madeira, J., Moreira, M., 2008. Evidências geológicas e geoquímicas para a existência de duas unidades estratigráficas distintas na Formação do Pico da Antónia (Ilha de Santiago, República de Cabo Verde). *Memórias e Notícias. Mus. Laboratório Miner. Geol. Univ. Coimbra* 3, 123–128.
- Martins, S., Mata, J., Munhá, J., Mendes, M.H., Maerschalk, C., Caldeira, R., Mattielli, N., 2010. Chemical and mineralogical evidence of the occurrence of mantle metasomatism by carbonate-rich melts in an oceanic environment (Santiago Island, Cape Verde). *Mineral. Pet.* 99, 43–65.
- Matos Alves, C.A., Macedo, J.R., Celestino Silva, L., Serralheiro, A., Peixoto Faria, A.F., 1979. Estudo geológico, petrológico e vulcanológico da ilha de Santiago (Cabo Verde). *Garcia Orta* 3, 47–74.
- McNutt, M., 1988. Thermal and mechanical properties of the Cape Verde Rise. *J. Geophys. Res. (Solid Earth)* 93 (B4), 2784–2794.
- Menendez, I., Silva, P.G., Martín-Betanco, I.M., Pérez-Torrado, F.J., Guillou, H., Scaillet, S., 2008. Fluvial dissection, isostatic uplift, and geomorphological evolution of volcanic islands (Gran Canaria, Canary Islands, Spain). *Geomorphology* 102, 189–203.
- Nelson, S.T., Tingey, D.G., Selck, B., 2013. The denudation of oceanic islands: the effects of climate, soil thickness, and water contact times on Oahu, Hawaii. *Geochimica Cosmochimica Acta* 103, 267–294.
- Nesbit, H.W., Markoviks, G., 1997. Weathering on granodioritic crust, long-term storage of elements in weathering profiles, and petrogenesis of siliciclastic sediments. *Geochimica Cosmochimica Acta* 61, 1653–1670.
- Nesbitt, H.W., Young, G.M., 1982. Early Proterozoic climates and plate motions inferred from major element chemistry of lutites. *Nature* 299, 715–717.
- Nichol, I., Garrett, R.G., Webb, J.S., 1966. Studies in regional geochemistry. *Trans. Inst. Min. Metallurgy* B75, 106–107.
- Palme, H., O'Neill, H.St.C., 2004. Cosmochemical estimates of mantle composition. In: Holland, H.D., Turrekian, K.K. (Eds.), *Treatise on Geochemistry*. Elsevier, pp. 1–38.
- Pett-Ridge, J.C., Monastra, V.M., Derry, L.A., Chadwick, O.A., 2007. Importance of atmospheric inputs and Fe-oxides in controlling soil uranium budgets and behavior along a Hawaiian chronosequence. *Chem. Geol.* 244, 691–707.
- Plant, J.A., Smith, D., Smith, B., Williams, L., 2001. Environmental geochemistry at the global scale. *Appl. Geochem.* 16, 1291–1308.
- Price, R.C., Gray, C.M., Wilson, R.E., Frey, F.A., Taylor, S.R., 1991. The effects of weathering on rare-earth element, Y and Ba abundances in Tertiary basalts from southeastern Australia. *Chem. Geol.* 93, 245–265.
- Prospero, J.M., Ginoux, P., Torres, O., Nicholson, S.E., Gill, T.E., 2002. Environmental characterization of global sources of atmospheric soil dust identified with the Nimbus 7 Total Ozone Mapping Spectrometer (TOMS) absorbing aerosols product. *Rev. Geophys.* 40, 1002. <http://dx.doi.org/10.1029/2000RG000095>.
- Rad, S., Louvat, P., Gorge, C., Gaillardet, K., Allégre, C.J., 2006. River dissolved and solid loads in the Lesser Antilles: new insight into basalt weathering processes. *J. Geochim. Explor.* 88, 308–312.
- Rad, S.D., Allegre, C.J., Louvat, P., 2007. Hidden erosion on volcanic islands. *Earth Planet. Sci. Lett.* 262, 109–124.
- Ramalho, R.A.S., 2011. *Building the Cape Verde Islands*. Springer.
- Ramalho, R.A.S., Quartau, R., Trenhaile, A.S., Mitchell, N.C., Woodroffe, C.D., Avila, S.P., 2013. Coastal evolution in oceanic islands: a complex interplay between volcanism, erosion, sedimentation and biogenic production. *Earth Sci. Rev.* 127, 140–170.
- Rapant, S., Rapošová, M., Bodíš, D., Marsina, K., Slaninka, I., 1999. Environmental-geochemical mapping program in the Slovak Republic. *J. Geochem. Explor.* 66, 151–158.
- Rawlins, B.G., McGrath, S.P., Scheib, A.J., Beward, N., Cave, M., Lister, T.R., Ingham, M., Gowing, C., Carter, S., 2012. *The Advanced Soil Geochemical Atlas of England and Wales*. British Geological Survey, Nottingham.
- Reimann, C., Siewers, U., Tarvainen, T., Bityukova, L., Eriksson, J., Gilucis, A., Gregoriuskiene, V., Lukashev, V.K., Matinian, N.N., Pasieczna, A., 2003. Agricultural Soils in Northern Europe: a Geochemical Atlas. *Geologisches Jahrbuch Schweizerbart'sche Verlagsbuchhandlung*, Stuttgart.
- Ren, L., Cohen, D.R., Rutherford, N.F., Zissimos, A.M., Morisseau, E.G., 2015. Reflections of the geological characteristics of Cyprus in soil rare earth element patterns. *Appl. Geochem.* 56, 80–93.
- Sanchez-Moreno, J.F., Mannaerts, C.M., Jetten, V., 2014. Rainfall erosivity mapping for Santiago island, Cape Verde. *Geoderma* 217–218, 74–82.
- Serralheiro, A., 1976. A Geologia da ilha de Santiago (Cabo Verde). *Bol. Mus. Laboratório Miner. Geol. Fac. Ciências Lisb.* 14, 157–369.
- Silva, L.C., Le Bas, M.J., Robertson, A.H.F., 1981. An oceanic carbonatite volcano on São Tiago, Cape Verde Islands. *Nature* 294, 644–645.
- Sleep, N., 1990. Hotspots and mantle plumes: some phenomenology. *J. Geophys. Res. (Solid Earth)* 95 (B5), 6715–6736.
- Tavares, J.P., Amiotte-Suchet, P., 2007. Rainfall erosion risk mapping in volcanic soils of Santiago Island, Cape Verde Archipelago. *Afr. Geosci. Rev.* 14, 399–414.
- Weltje, G.J., 2012. Quantitative models of sediment generation and provenance: state of the art and future developments. *Sediment. Geol.* 280, 4–20.
- Zhang, C., Pennington, J., 2004. African dry air outbreaks. *J. Geophys. Res. Atmos.* 109, D20108. <http://dx.doi.org/10.1029/2003JD003978>.